ELSEVIER

Journal of Molecular Catalysis A: Chemical 126 (1997) 151–159

JOURNAL OF MOLECULAR CATALYSIS A: CHEMICAL

The role of the metal during NO_2 reduction by C_3H_6 over alumina and silica-supported catalysts

Gratian R. Bamwenda *, Akira Obuchi, Atsushi Ogata, Junko Oi, Satoshi Kushiyama, Koichi Mizuno

National Institute for Resources and Environment, 16-3 Onogawa, Tsukuba, Ibaraki 305, Japan

Received 13 December 1996; revised 28 April 1997; accepted 15 May 1997

Abstract

The role of the metal during the reduction of NO_2 by propylene in oxygen over alumina and silica-supported gold, rhodium and platinum was studied. It was found that three parallel reactions take place, i.e., reduction of NO_2 to N_2 and N_2O, reduction of NO_2 to NO, and oxidation of propylene. It was also found that in the case of rhodium and platinum catalysts, the reaction may proceed entirely on metallic sites and that the alumina and silica supports do not play a critical role in determining the catalytic activity for NO_2 reduction. For gold catalysts, the reaction seems to involve a combination of metal and support catalyzed processes. It was noted that the selectivity toward N_2 formation seems to be primarily influenced by the nature of the metal. © 1997 Elsevier Science B.V.

Keywords: NO_2 reduction; Propylene; Rhodium; Platinum; Gold; Alumina; Silica supported catalyst

1. Introduction

The reduction of NO_x to N_2 is a subject of great interest, from both theoretical and practical aspects, as attempts are being made to get more insight into the nature of the active sites and to find catalysts and reaction conditions which would maximize the catalytic activity for the reduction of nitrogen oxides.

In the literature, the role played by different constituents of the catalysts in the reaction mechanism of NO_x reduction is still not clear because it seems to vary depending on the type of the reactant and the catalytic systems used. Another complicating factor is that it seems that different mechanisms may be operable with different catalysts [1–5].

In an attempt to address the fundamental question concerning the role of the metal in the mechanism of the selective catalytic reduction (SCR) of NO_x, we studied the reduction of NO_2 over alumina and silica-supported gold, rhodium, and platinum catalysts so as to gain insight into the possible role of metals during this process.

2. Experimental

2.1. Catalyst preparation

The gold, rhodium and platinum catalysts were prepared by impregnation of γ-Al_2O_3 (KHS-24 from Sumitomo Chemical, initially

* Corresponding author. Fax: +81-298-588259.

PII S1381-1169(97)00106-4

calcined in air at 600°C for 5 h, area 208 g m^{-2}) and silica (70–230 mesh, Merck) with aqueous solutions of $HAuCl_4 \cdot 4H_2O$, $RhCl_3 \cdot 3H_2O$ and $H_2PtCl_6 \cdot 6H_2O$, so as to yield 3 wt% metal loading. After impregnation, the slurries were freeze dried overnight at 15 Pa, then calcined in flowing air at 500°C for 5 h and finally reduced at 400°C under 1 vol% H_2 for 15 h. The resulting powders were sieved to give a 60–100 mesh fraction.

2.2. Catalyst characterization

The BET surface areas were determined using N_2 physisorption and a Nikkso 4232 analyzer. The dispersion of Pt and Rh were measured after activity tests by adsorption of CO using the pulse adsorption technique and the Ohkura R6015 system. The dispersion of Au particles was not determined due to the lack of an appropriate adsorbate.

Transmission electron micrographs (TEM) of the catalyst samples were obtained with a JOEL JEM-2000EX electron microscope. The metal particle size distributions were obtained from diameter measurements of up to 500 particles per catalyst sample from TEM photographic print enlargements, in a procedure similar to that we have reported previously [6]. The physicochemical properties of alumina supported catalysts are summarized in Table 1.

Table 1
Physicochemical properties of the catalysts

Catalyst	Surface area[a] (m^2/g)	Dispersion[b] (%)	d_{metal}[c] (nm)
γ-Al_2O_3	208	—	—
3% Au/Al_2O_3	177	n.d.[d]	54
3% Rh/Al_2O_3	172	75	0.9
3% Pt/Al_2O_3	164	34	1.0

[a] BET surface area.
[b] Determined by CO adsorption.
[c] Mean diameter of metal crystallites, determined from TEM micrographs (magnification: 400 000–2 000 000) by counting 100–500 particles for each sample.
[d] Not determined due to the lack of an appropriate adsorbate.

2.3. Catalytic measurements

The catalytic experiments were performed in a continuous flow tubular, quartz reactor (8 mm I.D.) operated at atmospheric pressure. The catalyst (200 mg) was packed into a 7–8 mm long bed between plugs of quartz wool. The feed consisted of the mixtures of ca. 1000 ppm NO_2, 1000 ppm C_3H_6, and 5% O_2, with a He (UHP) balance. The gas flow rates were controlled with mass flow controllers, and the total flow rate was maintained at 160 cm^3/min (STP), corresponding to a space velocity of ca. 27 000 h^{-1}. The feed gases was passed downward through the catalyst layer. After activity measurements at a given temperature, by bypassing the catalyst bed a background spectrum was measured to determine initial concentrations of NO, NO + NO_2, N_2O, CO and CO_2. The equilibrium for the reaction $NO_2 = NO + 1/2O_2$ is such that a small amount of NO and O_2 are always present in NO_2 at room temperature ($K_{298\,K} = 7.23 \times 10^{-7}$) [7]. Thus in the NO_2 feed, NO was initially present as a 0.6–1% impurity. The temperature was monitored by a thermocouple placed below the catalyst bed. The activity data were acquired at steady state, in an ascending temperature sequence followed by a descending temperature sequence. The obtained data had fairly good reproducibility.

2.4. Analysis

Total NO_x (NO + NO_2) in the feed and product streams was analyzed with a chemiluminescent NO_x analyzer (Yanagimoto, ECL-77A). The NO concentration was analyzed with a Horiba CLA-510SS analyzer. In repeated experiments, the product concentrations of nitrogen oxides were reproducible within ±5%.

The N_2, O_2 and CO in the effluent was sampled and analyzed by gas chromatography (GC) (Shimadzu, 14A) with a thermal conductivity detector (TCD), using 40 cm^3 min^{-1} He

as a carrier gas and a 2 m molecular sieve 13X column at 70°C. The outlet N_2O was analyzed both with a Horiba VIA-510 analyzer and by GC (Shimadzu GC-14B) equipped with a TCD detector and a 2 m stainless steel column packed with molecular sieves 13 × at 70°C. Carbon dioxide and CO in the products were analyzed with a non-dispersive infrared spectroscopic gas analyzer (Shimadzu, URA 106). The identification of the minor products was performed using a Hewlett Packard HP5970B GC-MS.

The following expressions will be used in the text. The conversion of NO_2 is defined as:

$$X_{NO_x} = \left([NO_2]_r + [NO]_r - [NO_2]_p - [NO]_p\right) / [NO_2]_r \times 100$$

Selectivity to $N_2 = [N_2]/([N_2] + [N_2O]) \times 100$.

Amount of carbon in C_3H_6 converted to CO_2 and CO: e.g.,

$$CO_2 = [CO_2]_p \times 100/3[C_3H_6]_r.$$

where $[NO_2]_r$ and $[NO_2]_p$ are reactor inlet and exit NO_x concentrations, respectively, and $[N_2]$ and $[N_2O]$ are the exit N_2 and N_2O concentrations, respectively.

3. Results

3.1. The $NO_2 = NO + 1/2O_2$ reaction in the absence of propylene

Fig. 1a shows the activities of the catalysts for NO_2 decomposition into NO. Nitrogen and N_2O were not detected in the product stream. For Rh and Pt catalysts, the conversion of NO_2 to NO increased with temperature and quickly attained equilibrium conversion levels at ca. 350°C and 400°C, respectively. At temperatures > 400°C, the thermodynamic equilibrium strongly favors the partial decomposition of NO_2 into NO and oxygen. This reaction was slow on Au and γ-Al_2O_3, and the conversions were always some distance from equilibrium. For Au/Al_2O_3, the temperatures required for the onset of NO_2 conversion to NO was > 350°C. Also, pure γ-Al_2O_3 significantly converted NO_2 to NO at temperatures > 400°C. The same results were obtained in repeated experiments with another batches of γ-Al_2O_3 and new reactors.

When the feed was a mixture of NO and O_2 (Fig. 1b), the oxidation of NO to NO_2 over Rh/Al_2O_3 and Pt/Al_2O_3 increased progressively with temperature passing over a maximum of 58 and 45% at ~ 350°C before declining to near equilibrium conversions of 44 and 42% at ca. 400°C, respectively. Only a slight oxidation of NO was observed on Au, peaking at about at 450°C. The γ-Al_2O_3 showed only a marginal activity in NO_2 formation and it was practically independent of temperature in the tested range.

It follows from Fig. 1 that in large excess of oxygen the equilibrium between NO_2 and NO is approached rapidly on Rh/Al_2O_3 and Pt/Al_2O_3 in the temperature range between 350–400°C, but Au/Al_2O_3 moves the reactants to equilibrium at temperatures > 500°C. The observed differences in the relative effectiveness of the catalysts for the $NO_2 = NO + 1/2O_2$ and its reverse reaction may possibly be ascribed to kinetic factors e.g., the differences in the dissociative adsorption rates of nitrogen oxides and oxygen, and the differences in the bonding strengths of the species formed on the catalysts surfaces. Finally, the results obtained in Fig. 1 suggest that the $NO_2 = NO + 1/2O_2$ forward and reverse reactions proceed on the same sites.

3.2. The $NO_2 + C_3H_6 + O_2$ reaction on alumina and silica-supported catalysts

The principal products from the $NO_2 + C_3H_6 + O_2$ reaction on both alumina and silica-supported catalysts were nitrogen, nitrous oxide, nitric oxide, carbon dioxide and carbon monoxide, and water. A variety of minor side-products such as cyanides, oxygenated products such as HCHO, CH_3CHO, C_2H_3CHO, $(CH_3)_2C{=}O$,

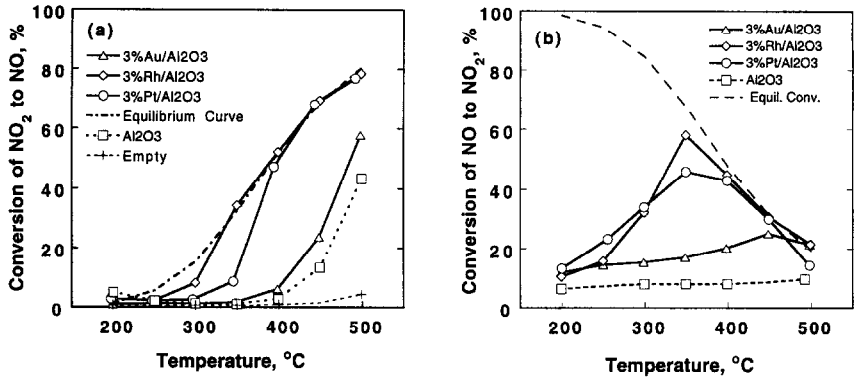

Fig. 1. Temperature dependence for (a) the NO_2 conversion to NO and (b) oxidation of NO to NO_2. Feed: (a) NO_2 = 1000 ppm, O_2 = 5%; (b) NO = 1000 ppm, O_2 = 5%, balance He. Flow rate, 160 cm^3/min; catalyst, 0.2 g. The dashed line is the equilibrium conversion.

and small amounts of cracked products such C_2H_4 and C_2H_6 were also present. A more detailed analysis of the minor products, and the variation of product distribution with temperature will be published elsewhere [8].

The catalytic effects on the selective reduction of NO_2 over alumina (solid lines) and silica (dashed lines)-supported catalysts are summarized in Figs. 2–5. The conversion of NO_2 over Pt and Rh supported on silica and alumina increased with temperature, reached a maximum at 250 and 300°C, respectively, and then declined sharply with increasing reaction temperature. Note that the maximum NO_x conversions are attained at lower temperatures than the temperature of maximum NO oxidation to NO_2, and the temperature where NO_2 decomposition into NO reaches equilibrium (see Fig. 1). The activity curve of the Au catalyst was markedly different from those of Rh and Pt. The NO_2 conversion increased steadily with temperature reaching conversions up to 52% at 400°C before gradually falling off with temperature [9]. The NO_2 conversion over γ-Al_2O_3 increased steadily with temperature and remained near 100% at temperatures > 400°C [10]. It is worth noting that although NO_2 conversion curves of γ-Al_2O_3 and Au/γ-Al_2O_3 are somewhat similar, γ-Al_2O_3 is far more effective than the Au/Al_2O_3 catalyst in the investigated temperature range. We will come back to this further in the text. In an empty reactor, not shown, there was practically no measurable NO_2 conversion below 500°C.

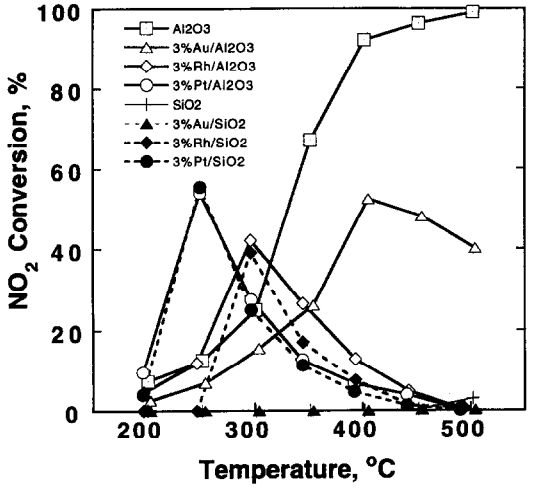

Fig. 2. Catalytic activities of silica (dashed line, closed symbol) and alumina (solid lines, open symbol)-supported 3 wt% Au, Rh and Pt for reduction of NO_2. Conditions: NO_2 = 970 ppm, C_3H_6 = 1000 ppm, O_2 = 5%, balance He. GHSV = 27000 h^{-1}.

The selectivity of N_2 and the undesirable N_2O production from NO_2 reduction are presented in Fig. 3. Platinum exhibited a poor selectivity to N_2, giving N_2O as a predominant product. The Au and Rh catalysts showed a good N_2 selectivity, while γ-Al_2O_3 reached N_2 selectivities ca. 90% at temperatures > 350°C. Overall, γ-Al_2O_3 and Au/γ-Al_2O_3 are more selective towards N_2 with a lower formation of N_2O.

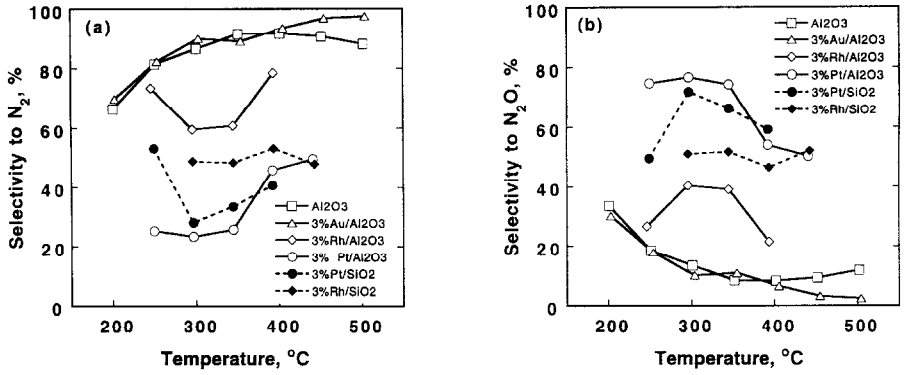

Fig. 3. Selectivity of NO_2 conversion to N_2 and N_2O. Conditions as in Fig. 2.

Fig. 4 depicts the yield of CO and CO_2 from the conversion of C_3H_6 during the reduction of NO_2. It is seen that on Au, Rh and Pt catalysts, at temperatures greater than the optimum temperature, the combustion of C_3H_6 becomes a predominant route. A notable feature here is the simultaneous enhanced evolution of the C_3H_6 oxidation products CO_2 and CO, and the onset of the NO_2 conversion (see Fig. 2). Although γ-Al_2O_3 was able to convert NO_2 to N_2 it gave mainly CO in the process. A careful examination of Figs. 2 and 4 reveals that the low NO_2 conversion over Au/Al_2O_3 in comparison with bare Al_2O_3 can be attributed to the fact that at a substantial amount of propylene is burned over Au/Al_2O_3 before it can selectively reduce NO_x, and this leads to the suppression of its activity.

Fig. 5 shows the conversion of NO_2 to NO from the $NO_2 + C_3H_6 + O_2$ reaction as a function of temperature. At low temperatures, a high conversion of NO_2 to NO, above equilibrium $NO_2 \rightarrow NO + 1/2O_2$ conversion, was noted on Au, Rh and Pt catalysts. With increase in reaction temperature, the NO composition eventually approached the equilibrium between 350–400°C on alumina-supported catalysts and, at ca. 400°C over silica-supported catalysts. On Au/Al_2O_3, the NO yield fell below equilibrium concentrations at temperatures greater than the temperature of maximum NO_2 conversion (see Fig. 2). Over pure Al_2O_3, the NO yield was far below equilibrium and it remained more or less constant before declining at temperatures > 350°C. Nearly the same conversions to NO

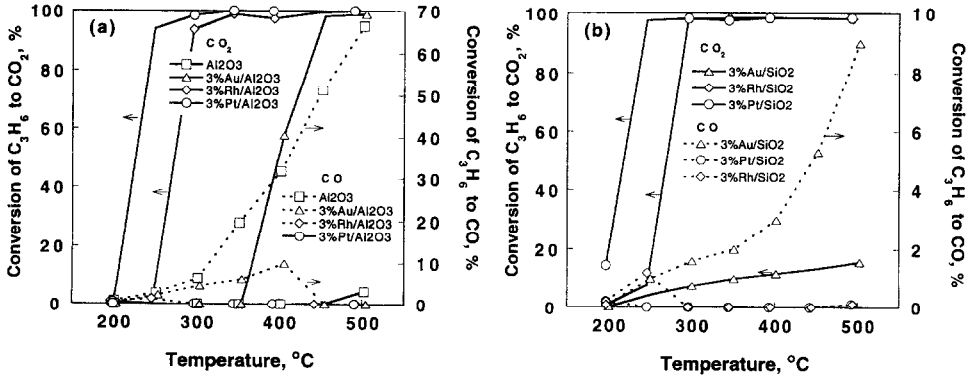

Fig. 4. Conversion of C_3H_6 to CO and CO_2 as a function of temperature. Conditions as in Fig. 2.

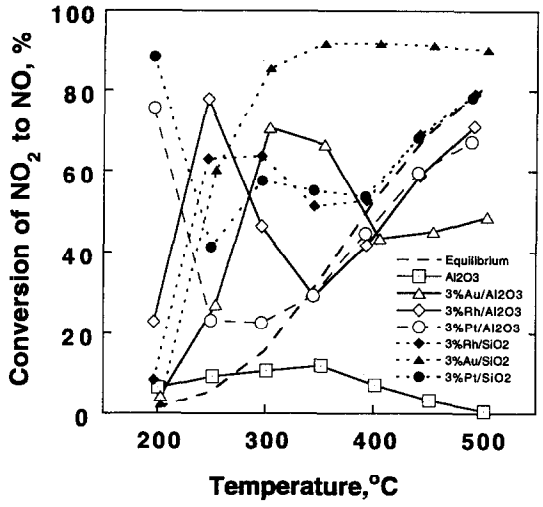

Fig. 5. Conversion of NO_2 to NO during the SCR of NO_2. Conditions as in Fig. 2.

were obtained in runs in which the reaction temperature was raised to 500°C and lowered again to 200°C.

It is evident from Figs. 2–5 that the temperature-dependent behavior, the percentage conversions of NO_2 reduction to N_2 for alumina- and silica-supported Rh and Pt catalysts are qualitatively quite similar; the most notable differences are that the measurable conversion set in at lower temperatures on alumina-supported catalysts than on silica-supported catalysts, and the disparity in the selectivity toward N_2 formation; Rh catalysts exhibiting higher N_2 yields. Thus, it appears that alumina and silica has little, if any, direct effect on the NO_2 reduction process over these catalysts. Surprisingly, only a minute activity was observed over Au/SiO_2 and none on bare SiO_2 at temperatures up to 500°C.

3.3. The $NO + C_3H_6 + O_2$ reaction

In order to get the full picture on the reduction of nitrogen oxides over these catalysts, we studied the $NO + C_3H_6 + O_2$ reaction under identical reaction conditions, and the results are summarized in Table 2. In the case of Rh and Pt catalysts, the qualitative comparison between the $NO + C_3H_6 + O_2$ and $NO_2 + C_3H_6 + O_2$ systems indicates similar behaviors from the point of view of both products observed and the temperature of maximum activity. For Au/Al_2O_3 and unsupported Al_2O_3, the conversion levels were lower than when the feed stream was $NO_2 + C_3H_6 + O_2$, but here the conversion levels of NO on Au/Al_2O_3 was significantly higher than that of bare Al_2O_3. This result partially indicates that over bare alumina and Au/Al_2O_3, NO_2 plays a certain role in the reduction of NO. The results presented in Fig. 3 and Table 2 also suggest that the selectivity with respect to N_2 seems to be primarily influenced by the nature of the metal used.

Table 2
Catalytic activities and products from the $NO + C_3H_6 + O_2$ reaction

Catalyst	T^a_{max} (°C)	Conversion (%)		Selectivity (%)		Yield of NO_2 (%)
		NO	C_3H_6	N_2	N_2O	
γ-Al_2O_3	500	34	69	97	3	5
3% Au/Al_2O_3	450	41	94	94	6	4
3% Rh/Al_2O_3	300	44	98	62	38	21
3% Pt/Al_2O_3	250	49	99	42	58	16
3% Au/SiO_2	450	2	10	89	11	6
3% Rh/SiO_2	300	40	99	54	46	14
3% Pt/SiO_2	250	58	99	44	56	5

Conditions: NO = 940–970 ppm, C_3H_6 = 1000 ppm, O_2 = 5%, balance He. GHSV = 27000 h^{-1}.
[a]Temperature of maximum NO conversion.
No measurable activity was detected on bare silica.

4. Discussion

The purpose of this study was to obtain information concerning the catalytic reduction of NO_2 and to investigate the role played by the metal during the SCR process.

From the results presented above, the tested catalysts can be divided into catalysts that are active at low temperatures (Pt/Al_2O_3 and Rh/Al_2O_3) and those active at relatively high temperatures (Al_2O_3, Au/Al_2O_3).

4.1. Pure Al_2O_3

During the SCR of NO_2, γ-alumina has exhibited a significant activity towards NO_2 reduction to N_2, and NO_2 partial decomposition into NO. This may be rationalized in the terms of the following considerations: The surface of γ-Al_2O_3 possesses both Lewis acid and basic sites which have been confirmed by strong adsorption of basic and acidic molecules [11]. Propylene can be activated on γ-Al_2O_3 through the interaction with Lewis acid sites and/or by the concerted action of the basic and acidic sites to form allyl complexes [12,13]. The interaction of these adspecies with gas phase or adsorbed NO and NO_2 complexes may lead to the formation of active intermediates which may eventually lead to the formation of the observed products. Recently, Sadykov et al. [14] provided experimental evidence that stable nitrates, as M–NO_3 or M–ONO_2, were adsorbed on γ-Al_2O_3 and suggested that the interaction of these strongly bound nitrogen oxides species with activated hydrocarbons provide the selective reduction route observed on γ-Al_2O_3.

4.2. Pt supported on γ-Al_2O_3 and SiO_2

The remarkable feature of the data from platinum catalysts is the great similarity in the NO_2 conversion results over Pt supported on alumina and on inactive silica. The peak NO_2 conversion and kinetic behavior of Pt/Al_2O_3 are very similar to those of Pt/SiO_2; it seems that, on Pt-based catalysts, the SCR reaction may proceed predominantly on active centers of platinum crystallites of the catalysts. In other words, the support component contributes little to the SCR of NO_2. The high NO yields observed from the SCR of NO_2 at lower temperatures may be ascribed to the fact that, apart from the direct decomposition of NO_2 shown in Fig. 1a, NO is additionally produced from the interaction between adsorbed propylene and NO_2. Nitrogen dioxide has an unpaired electron. It is known that NO_2 radicals can remove hydrogen from saturated hydrocarbons, e.g., during the nitration of CH_4 to form nitromethane via a gas phase $NO_2 + CH_4$ reaction [15,16]. Thus, it seems reasonable to speculate that during NO_2 reduction, NO_2 can abstract an allylic hydrogen from propylene to form NO, OH, propenyl and/or allyl radicals, which may eventually take part directly or indirectly in subsequent NO_2 reduction reactions.

As is evident from Figs. 2 and 4, the NO_2 reduction activity over platinum-based catalysts passed through the maximum as the conversion of C_3H_6 to CO_x increased and approached a 100% level. This demonstrates that part of the C_3H_6 conversion process is initiated by the interaction between NO_2 and C_3H_6 species, as described above. After passing the peak activity, the NO_2 reduction activity falls with increasing reaction temperature. The following explanations can be sought for this behavior. At temperatures higher than optimum temperature, the fall in activity of Pt catalysts is related to the decrease in surface coverage by nitrogen oxides or its complexes, i.e., nitrites and/or nitrates, and a decrease in organic adspecies due to desorption and/or decomposition. These factors decrease the NO_2 reduction rate, as we have observed previously from in situ DRIFT spectroscopy studies [17,18]. Another explanation is the competition for propylene between oxygen (combustion process) and NO_x species. A higher temperature favors the C_3H_6 combustion.

4.3. Rh supported on γ-Al_2O_3 and SiO_2

The trend and performance of Rh/Al_2O_3 were similar to that observed for Rh/SiO_2. The NO_2 SCR reaction profile for rhodium catalysts was much the same to that observed in the case of alumina and silica supported-platinum catalysts. A notable exception is that Rh catalysts displayed a slightly wide activity window with a temperature of maximum NO_2 reduction ca. 50°C higher than that of Pt catalysts, and they provided a better N_2 selectivity in the whole temperature range examined. Similar activity trends were noted in the $NO + C_3H_6 + O_2$ reaction (not shown). Therefore, the observed catalytic behavior of Rh catalysts can be explained on the similar basis as that discussed above for Pt catalysts.

When considering the commercial application of Rh and Pt catalysts, it would be important to minimize the formation of N_2O which contributes to both stratospheric ozone destruction and greenhouse warming [19,20].

At the temperature of maximum NO_2 conversion, the N_2/N_2O concentration ratio in the exit stream was about 0.3 and 1.6 for Pt and Rh catalysts, respectively. In the $NO + C_3H_6 + O_2$ reaction, the N_2/N_2O ratio was 0.6 and 1.6, for Pt and Rh catalysts, respectively (Table 2). Thus, for Rh catalysts, the selectivity to N_2 was nearly identical for the $NO_2 + C_3H_6 + O_2$ and $NO + C_3H_6 + O_2$ systems, whereas over Pt catalysts it was slightly better in the $NO + C_3H_6 + O_2$ system. The better selectivity to N_2 observed on Rh catalysts can be attributed to the fact that Rh catalysts have a good activity for N_2O decomposition to dinitrogen. When we used the same Pt and Rh catalysts, to investigate the N_2O (0.1%) + O_2 (5%)/He reaction, the steady-state rates for N_2O decomposition were 3.6 and 5.7 $\times 10^3$ μmol(N_2O) g^{-1} h^{-1} for 3% Pt/Al_2O_3 and 3% Rh/Al_2O_3 at 300°C, respectively. At 400°C, the N_2O decomposition rates were 20 and 24.4 $\times 10^3$ μmol g^{-1} h^{-1} for 3% Pt/Al_2O_3 and 3% Rh/Al_2O_3, respectively. On 3% Rh/Al_2O_3, the temperature of 50% (T_{50}) decomposition of N_2O for the $N_2O + O_2$ reaction was ca. 400°C [21,22]. Thus, the N_2O decomposition performance of Pt/Al_2O_3 is negligible in comparison to that of Rh/Al_2O_3. Therefore, the observed differences in the N_2/N_2O ratio between Pt and Rh catalysts during the SCR of NO_2 may be interpreted on the basis of the fact that Rh exhibits a significantly higher activity for the decomposition of N_2O to N_2 than Pt catalysts.

Work is underway in our laboratory to develop catalysts for N_2O decomposition after a NO_x reduction stage. Preliminary results show that hydrotalcit derived catalysts, e.g., ZnAlRh–HTlc (0.8 wt% Rh) with a T_{50} = 350°C, are prospective candidates for practical application even in the presence of water [22]. With such a catalyst, the overall conversion of NO_x to N_2 can be improved and catalytic efficiencies of industrial relevance can be obtained.

4.4. Au supported on γ-Al_2O_3 and SiO_2

The impregnation of gold on alumina slightly enhanced the activity for oxidation of NO to NO_2 (Fig. 1b), and led to the formation of a relatively large amount of NO during the SCR of NO_2 than that noted over bare alumina (Fig. 5). Over Au/SiO_2, mainly a non-selective interaction between C_3H_6 and NO_2 leading to the formation of NO and O_2 was noted; only a negligible NO_2 reduction activity to N_2 was observed. The fact that the activity of Au/Al_2O_3 towards NO_2 reduction was lower than that observed over bare Al_2O_3 implies that gold on the alumina masks some of the sites on the alumina and makes them inactive for reduction of NO_2. On the other hand, Au/Al_2O_3 displayed a better activity in the $NO + C_3H_6 + O_2$ reaction. In this case, it appears reasonable to assume that, the reaction may involve a combination of metal and support catalyzed processes, where Au assists Al_2O_3 in the formation of NO_2, which is then mostly reduced to N_2 and small amounts of N_2O on active sites of Al_2O_3. It may be added here that, the fact that the SCR

of NO_2 proceeds at such reasonable rate in spite of much of the NO_2 being converted to NO suggests that the propagation of the NO_x reduction may take place via an interaction between activated C_3H_6 species and either NO or NO_2.

5. Summary

The Rh and Pt catalysts showed a relatively high NO_2 reduction activity in the 250–300°C temperature range but with a narrow temperature window over which the catalysts are effective. Gold and alumina showed a low activity towards NO_2 decomposition in the absence of propylene, moderate SCR activities at high temperatures with a broad temperature window, and a remarkably high NO_2 conversion selectivity to N_2 as compared with N_2O.

The kinetic behavior and performances of Rh/Al_2O_3 and Pt/Al_2O_3 are very similar to that of Rh/SiO_2 and Pt/SiO_2 indicating that, in the case of Rh and Pt catalysts, the supports Al_2O_3 and SiO_2, contribute little to the catalytic activity for NO_2 reduction. The important factor appears to be the reaction dynamics between competing reactions, e.g., between the reduction of NO_2 to N_2 and N_2O, NO_2 partial decomposition to NO and, combustion of propylene on the surfaces of rhodium and platinum or their oxides. In the case of gold catalysts, the reaction may involve a combination of metal and support catalyzed processes.

Since the both $NO_2 + C_3H_6 + O_2$ and $NO + C_3H_6 + O_2$ reactions proceed at comparable rates over Rh and Pt, this suggests that the oxidation of NO to NO_2 is not a prerequisite for the SCR reaction to proceed over Pt and Rh metals. Such an initial NO pre-oxidation step seems to be necessary on catalysts like alumina or alumina-supported gold.

Finally, the present results also suggest that the selectivity with respect to N_2 seems to be primarily influenced by the nature of the metal used.

References

[1] M. Iwamoto, Catal. Today 29 (1996) 29.
[2] T. Tanaka, T. Okuhara, M. Misono, Appl. Catal. 4 (1994) L1.
[3] R.H.H. Smits, Y. Iwasawa, Appl. Catal. 6 (1995) L201.
[4] M. Inaba, Y. Kintaichi, H. Hamada, Catal. Lett. 36 (1996) 223.
[5] R. Burch, P.J. Millington, A.P. Walker, Appl. Catal. B 4 (1994) 65.
[6] G.R. Bamwenda, S. Tsubota, T. Nakamura, M. Haruta, J. Photochem. Photobiol. A: Chem. 89 (1995) 177.
[7] J.H. Lunsford, J. Colloid Interface Sci. 26 (1968) 355.
[8] G.R. Bamwenda, A. Obuchi, A. Ogata, J. Oi, S. Kushiyama, K. Mizuno, to be published.
[9] A. Ueda, T. Oshima, M. Haruta, in: G. Centi, C. Cristiani, P. Forzatti, S. Perathoner (Eds.), Environmental Catalysis, SCI Pub., Rome, 1995, p. 343.
[10] H. Hamada, Y. Kintaichi, M. Sasaki, T. Ito, M. Tabata, Appl. Catal. 70 (1991) L15.
[11] H. Knozinger, Adv. Catal. Relat. Subj. 25 (1976) 184.
[12] J. Kubota, T. Ohtani, J.N. Kondo, C. Hirose and K. Domen, Proceed. International Symposium on Surface Nano-Control of Environmental Catalysts and Related Materials, Tokyo, 1996, p. 175.
[13] V.F. Kiselev, O.V. Krylov (Eds.), Adsorption and Catalysis on Transition Metals and their Oxides. Springer Series in Surface Science 9 (1989) 211.
[14] V.A. Sadykov, S.L. Baron, V.A. Matyshak, G.M. Alikina, R.V. Bunina, A. Ya Rozovskii, V.V. Lunin, E.V. Lunia, A.N. Kharlanov, A.S. Ivanova, S.A. Veniaminov, Catal. Lett. 37 (1996) 157.
[15] G.A. Olah, R. Malhotra, C.N. Suhash, Nitration Methods and Mechanisms, VCH, New York, 1989.
[16] Y. Li, T.L. Slanger, J.N. Armor, J. Catal. 150 (1994) 388.
[17] G.R. Bamwenda, A. Obuchi, A. Ogata, K. Mizuno, Chem. Lett., (1994) 2109.
[18] G.R. Bamwenda, A. Obuchi, A. Ogata, J. Oi, K. Mizuno, Appl. Catal. B Environ. 6 (1995) 311.
[19] B. Bolin, B.A. Doos, J. Jager, R.A. Warrick, (Eds.), The Greenhouse Effect, Climate Change, and Ecosystems, John Wiley, NY, 1986.
[20] National Research Council, Causes and Effects of Stratospheric Ozone Reduction: An update, National Academy Press, Washington, DC, 1982.
[21] J. Oi, A. Obuchi, A. Ogata, H. Yagita, G.R. Bamwenda, K. Mizuno, Chem. Lett. (1995) 453.
[22] J. Oi, A. Obuchi, A. Ogata, H. Yagita, G.R. Bamwenda, K. Mizuno, Appl. Catal. B 12 (1997) 277–286.